Wu *et al. J Wood Sci* (2021) 67:56
https://doi.org/10.1186/s10086-021-01988-2

Journal of Wood Science

ORIGINAL ARTICLE

Open Access

Comparison of colors, microstructure, chemical composition and thermal properties of bamboo fibers and parenchyma cells with heat treatment

Jieyu Wu[1,2], Tuhua Zhong[3], Wenfu Zhang[4*], Jiangjing Shi[1,2], Benhua Fei[3] and Hong Chen[1,2*]

Abstract

The effects of heat treatment at various temperatures on mechanically separated bamboo fibers and parenchyma cells were examined in terms of color, microstructure, chemical composition, crystallinity, and thermal properties. The heat-treated parenchyma cells and fibers were characterized by scanning electron microscopy (SEM), Fourier-transform infrared spectroscopy (FTIR), chemical composition analysis, and thermogravimetric analysis (TGA). The results revealed that the colors of bamboo fibers and parenchyma cells were darkened as treatment temperature increased. The microstructure of the treated fibers and parenchyma cells slightly changed, yet the shape of starch granules in parenchyma cells markedly altered at a temperature of above 160 °C. The chemical compositions varied depending on the heat treatment temperature. When treated at 220 °C, the cellulose content was almost unchanged in fibers but increased by 15% in parenchyma cells; the hemicellulose content decreased and the lignin content increased regardless of fibers and parenchyma cells. The cellulose crystal structure was nearly unaffected by heat treatment, but the cellulose crystallinity of fibers changed more pronouncedly than that of parenchyma cells. The thermal stability of parenchyma cells after heat treatment was affected more substantially compared to fibers.

Keywords: Bamboo, Parenchyma cells, Fibers, Heat treatment, Color, Microstructure

Introduction

Bamboo powder has been considered as one of the most suitable fillers for plastic composite because of their impressive features, for example, renewable, cost-effective, environmentally benign, and high modulus yet low density [1]. Bamboo plastic composites have been widely used for flooring, furniture and so on [2, 3]. To further reduce water absorption and improve mechanical properties, bamboo powder is usually pretreated with acid, alkali, coupling agent, carbonize, etc. [3–6]. However, the above pretreatments often involve chemical usage, probably leading to environmental pollution. Therefore, a cost-effective and environmentally friendly heat treatment is widely adopted by the bamboo industry to obtain high-performance bamboo [7–10].

Bamboo powder for bamboo plastic composite is usually ground from the whole bamboo directly. However, bamboo is made up of approximately 50% parenchyma cells, 40% fibers, and 10% vascular bundles (vessels, sieve tubes with companion cells) [11]. Bamboo fibers and parenchyma cells have an apparent discrepancy in microstructure, chemical composition, and performance [12, 13]. Bamboo fibers had higher cellulose and lignin contents, but lower hemicellulose content when compared with parenchyma cells [14]. The cellulose crystallinity in fibers was higher than that of parenchyma cells

*Correspondence: zhangwenfu542697@163.com; chenhong@njfu.edu.cn
[1] College of Furnishings and Industrial Design, Nanjing Forestry University, Nanjing 210037, China
[4] Zhejiang Academy of Forestry, Hangzhou 310023, China
Full list of author information is available at the end of the article

[12, 15]. Bamboo fibers had a straight shape with a thick cell wall and small lumen, while the parenchyma cells had an oval shape with a thin cell wall and large, hollow cell cavities which usually stored starch [16]. The variation in structures and chemical compositions often result in property discrepancies between bamboo fibers and parenchyma cells [15]. For example, the thermal stability of fibers was higher than that of parenchyma cells in bamboo [17]. Therefore, the property variation of fibers and parenchyma cells after pretreatment may affect their filled composites to different extents. To date, there was little research reporting on the direct comparison of the heat treatment effects between sole fibers and sole parenchyma cells in terms of color, microstructure, and chemical compositions. In this regard, getting more insight into the heat-induced difference between bamboo fibers and parenchyma cells may help elucidate which one was influenced pronouncedly when melt-blending with plastics at high temperatures.

In this study, bamboo fibers and parenchyma cells mechanically isolated from each other were treated at various heating temperatures in an oven. The heating-induced discrepancy between fibers and parenchyma cells in terms of morphology, microstructure, chemical composition, and thermal stability was examined by scanning electron microscopy (SEM), Fourier-transform infrared spectroscopy (FT-IR), X-ray diffraction (XRD), and thermogravimetric analysis (TGA).

Materials and methods

Materials

Three-year-old Moso bamboos (*Phyllostachys heterocycla*) were harvested from Zhejiang Province, China. The parenchyma cells and fibers were prepared, as schematically depicted in Fig. 1. The bamboo culms were chopped into bamboo rings and ground into powder. The size of bamboo powder is shown in Table1. The bamboo powder was placed in water and stirred for 5 min. Due to the difference in density, the parenchyma cells floated on the water and the fibers precipitated at the bottom. The fibers and parenchyma cells were collected separately followed by oven drying at 50 °C for 5 h. Finally, the fibers and parenchyma cells were treated at 100, 120, 140, 160, 180, 200, and 220 °C for 6 h in the oven.

Table 1 The proportion of different mesh number of bamboo powder

Mesh number	Proportion (%)
60–100	31.11
100–140	34.07
140–180	24.19
≥ 180	10.64

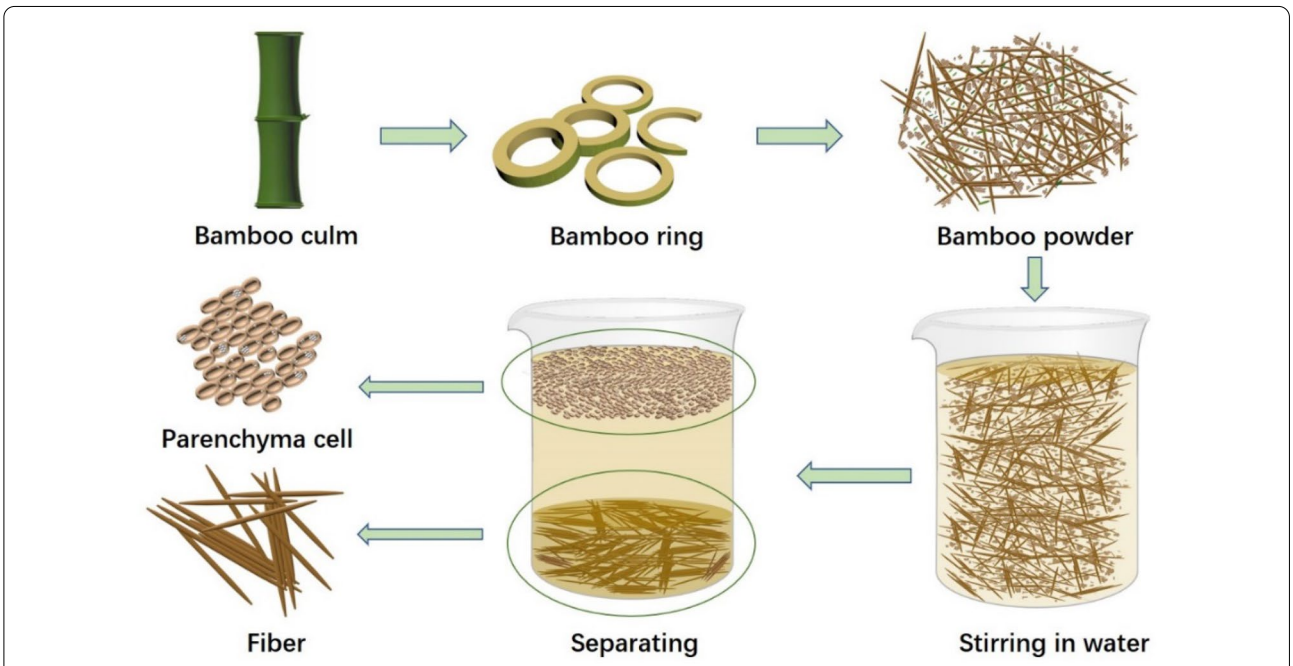

Fig. 1 The separation of parenchyma cells and fibers from bamboo

Characterizations

Color and microstructure

Color parameters were measured with a SEGT-J portable colorimeter. Three replicates were measured for each sample. The CIE lab system was characterized by three parameters, L^*, a^*, and b^*. The lightness (L^*) ranged from 0 to 100, and the greater the value of L, the brighter the surface of the material. a* was defined as the red/green coordinate, $+a^*$ was the red direction, and $-a^*$ was the green direction. b^* defined as the yellow/blue coordinate, $+b^*$ was the yellow direction, and $-b^*$ was the blue direction [18, 19]. The lightness difference (ΔL^*), red/green difference (Δa^*), yellow/blue difference (Δb^*) and the color difference (ΔE^*) were calculated according to the following Eqs. (1–4):

$$\Delta L^* = L^*_{\text{heated}} - L^*_{\text{untreated}}, \tag{1}$$

$$\Delta a^* = a^*_{\text{heated}} - a^*_{\text{untreated}}, \tag{2}$$

$$\Delta b^* = b^*_{\text{heated}} - b^*_{\text{untreated}}, \tag{3}$$

$$\Delta E^* = [(\Delta L^*)^2 + (\Delta a^*)^2 + (\Delta b^*)^2]^{1/2}. \tag{4}$$

The microstructure of the untreated- and heat-treated parenchyma cells and fibers was observed with an emission scanning electron microscopy (ESEM, Quanta 200, FEI Company, USA). The morphology of starch was observed by a cold field scanning electron microscopy (Regulus 8100, Hitachi Company, Japan).

Chemical composition and thermogravimetric analysis (TGA)

The FTIR spectra of the heat-treated parenchyma cells and fibers were recorded by a spectrometer (VERTEX 80 V, Bruker, Germany) within the range of 4000–500 cm^{-1} at a resolution of 4 cm^{-1} and 64 scans. Three replicates were measured for each sample. The chemical composition of the untreated- and heat-treated parenchyma cells and fibers was determined according to the National Renewable Energy Laboratory (NREL) procedures [20]. The sugars hydrolyzed from cellulose and hemicellulose were analyzed by high-performance liquid chromatography (HPLC) 1260 system equipped with an Aminex HPX-87H column (300 × 7.8 mm) and a refractive index (RI) detector. Acid-soluble lignin content was analyzed with a UV–visible spectrophotometer at 205 nm. The content of insoluble lignin was determined by drying the solid at 105 ± 3 °C to constant weight and burning in a muffle furnace at 575 ± 25 °C.

The crystallinity of the untreated and heat-treated parenchyma cells and fibers was examined by an X-ray diffractometer with a CuKα radiation source (XRD, Ultima IV, Rigaku, Japan). The crystallinity index (CrI) was the relative crystallinity, I_{200} was the maximum intensity of the (200) diffraction peak, and I_{am} was the amorphous diffraction intensity. The crystallinity index was calculated by the following Formula (5):

$$\text{CrI} = \frac{I_{200} - I_{\text{am}}}{I_{200}} \times 100\%. \tag{5}$$

The thermal stability and degradation behavior of the untreated- and heat-treated parenchyma cells and fibers were examined by a thermogravimetric analyzer (TGA, STA409PC, Netzsch, Germany).

Results and discussion

Color changes

The color of the heat-treated parenchyma cells and fibers is exhibited in Fig. 2. Both fibers and parenchyma cells were increasingly darkened when treated with increasing heat temperature. Heat temperature above 160 °C rendered an apparent impact on the color of both parenchyma cells and fibers. Besides, the rougher surface of parenchyma cells was observed compared to

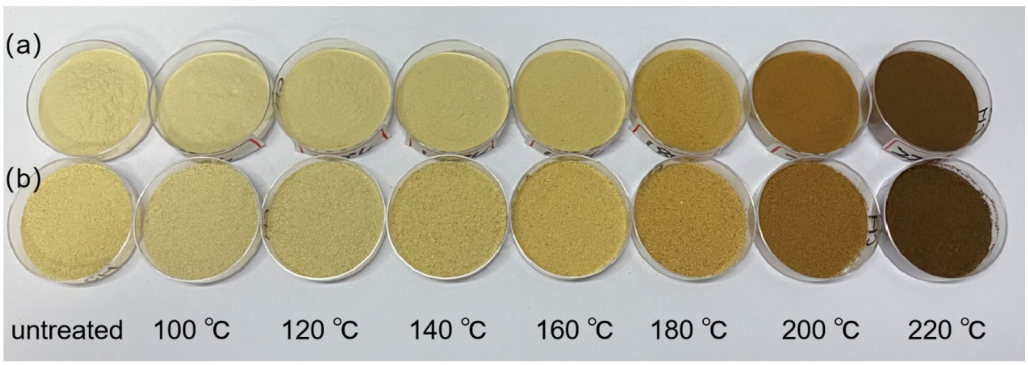

Fig. 2 The color of the heat-treated **a** fibers and **b** parenchyma cells

fibers, this might be largely attributed to the rupture of parenchyma cells and the breakdown of cell cavities during the sample preparation [15].

Figure 3 shows the color parameters of the untreated and heat-treated fibers and parenchyma cells. ΔL^* in both treated fibers and parenchyma cells increased abruptly when treated at above 160 °C, the ΔL^* for parenchyma cells changed more pronouncedly when compared with fibers. It indicated that the lightness of heat-treated parenchyma cells and fibers declined as temperature increased. The ΔE^* values in both fibers and parenchyma cells increased slightly below the temperature of 160 °C, but increased sharply for fibers and parenchyma cells when temperature increased beyond the point at 160 and 140 °C, respectively. The trend of the Δa^* and Δb^* values for fibers and parenchyma cells changed similarly. The Δa^* and Δb^* values decreased firstly and then increased, the turning point in fibers and parenchyma cells was 160 and 120 °C, respectively, but finally decreased at 220 °C. The fibers were greenish and bluish when heated below 160 °C, but became reddish and yellowish at above 160 °C. However, the marked change in color for parenchyma cells occurred at 120 °C. In addition, the color of fibers and parenchyma cells became bluish and a little reddish when treated at 220 °C. The trend in the color change induced by heat for separate parenchyma cells and fibers was consistent with the reported phenomenon for bulk bamboo strips and bamboo fiber bundles in previous work [7, 10, 21, 22].

Microstructure

The microstructure of the parenchyma cells and fibers after the heat treatment is exhibited in Fig. 4. The parenchyma cells were broken during the sample preparation process, the starch existing in the parenchyma cells' cavity was exposed (Fig. 4f). The microstructure of fibers and parenchyma cells was not remarkably altered by heat treatments.

Starch granules in the untreated- and treated parenchyma cells are presented in Fig. 5. The morphology of starch granules was altered significantly by heat. The untreated starch granule in the parenchyma cell was round or oval and the surface was smooth. The surface rendered a spike-like shape when treated at 160 °C or higher (Additional file 1: Figs. S1 and S2), and the number of starch granules with such shapes and morphology went up with increasing temperature.

The morphology of starch granules in the parenchyma cells treated by heat was different from that of the heat-treated glutinous rice starches but similar to that of corn starch granules treated by high pressure [23–25]. The surface of glutinous rice starch was rough and appeared with aggregations, irregular sizes, uneven shapes, and tight connections. Corn starch granules collapsed and became doughnut-shaped after

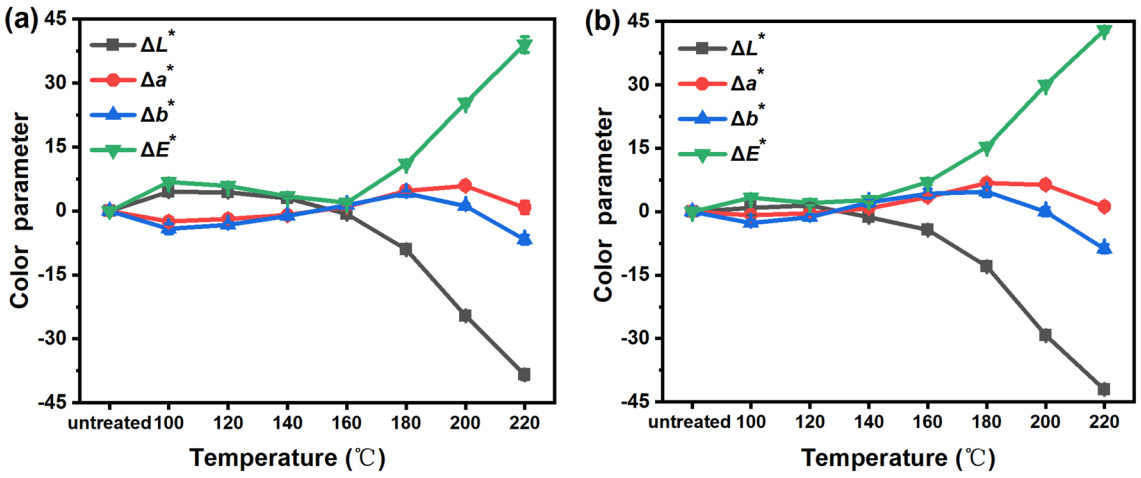

Fig. 3 Changes in color parameters of **a** fibers and **b** parenchyma cells

(See figure on next page.)

Fig. 4 SEM images of the microstructure of **a** the untreated fiber, **b** the120 ℃-treated fiber, **c** the160 ℃-treated fiber, **d** the 180 ℃-treated fiber, **e** the 220 ℃-treated fiber, **f** the untreated parenchyma cell, **g** the 120 ℃-treated parenchyma cell, **h** the 160 ℃-treated parenchyma cell, **i** the 180 ℃ treated parenchyma cell, **j** the 220 ℃-treated parenchyma cell

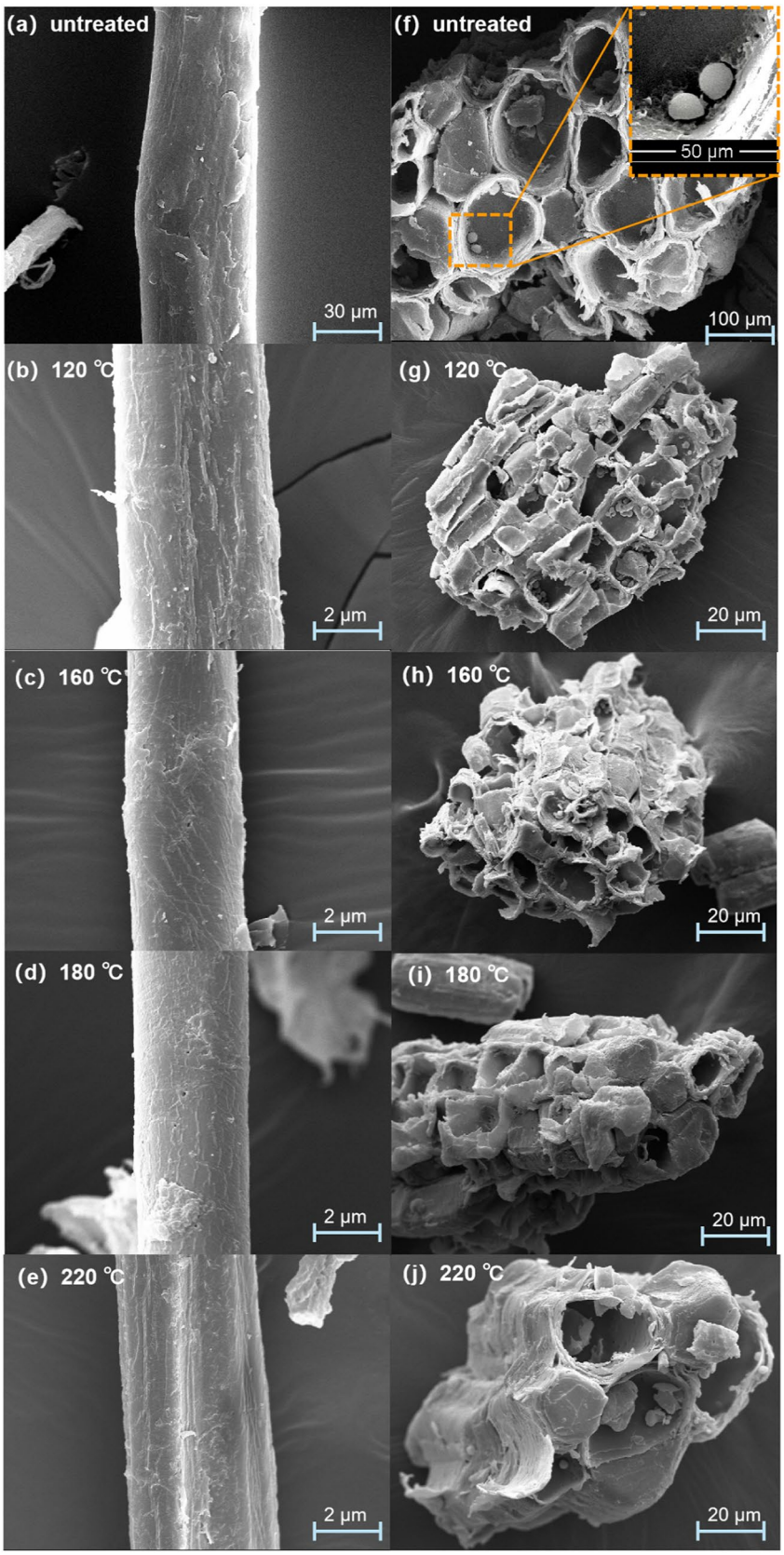

Fig. 4 (See legend on previous page.)

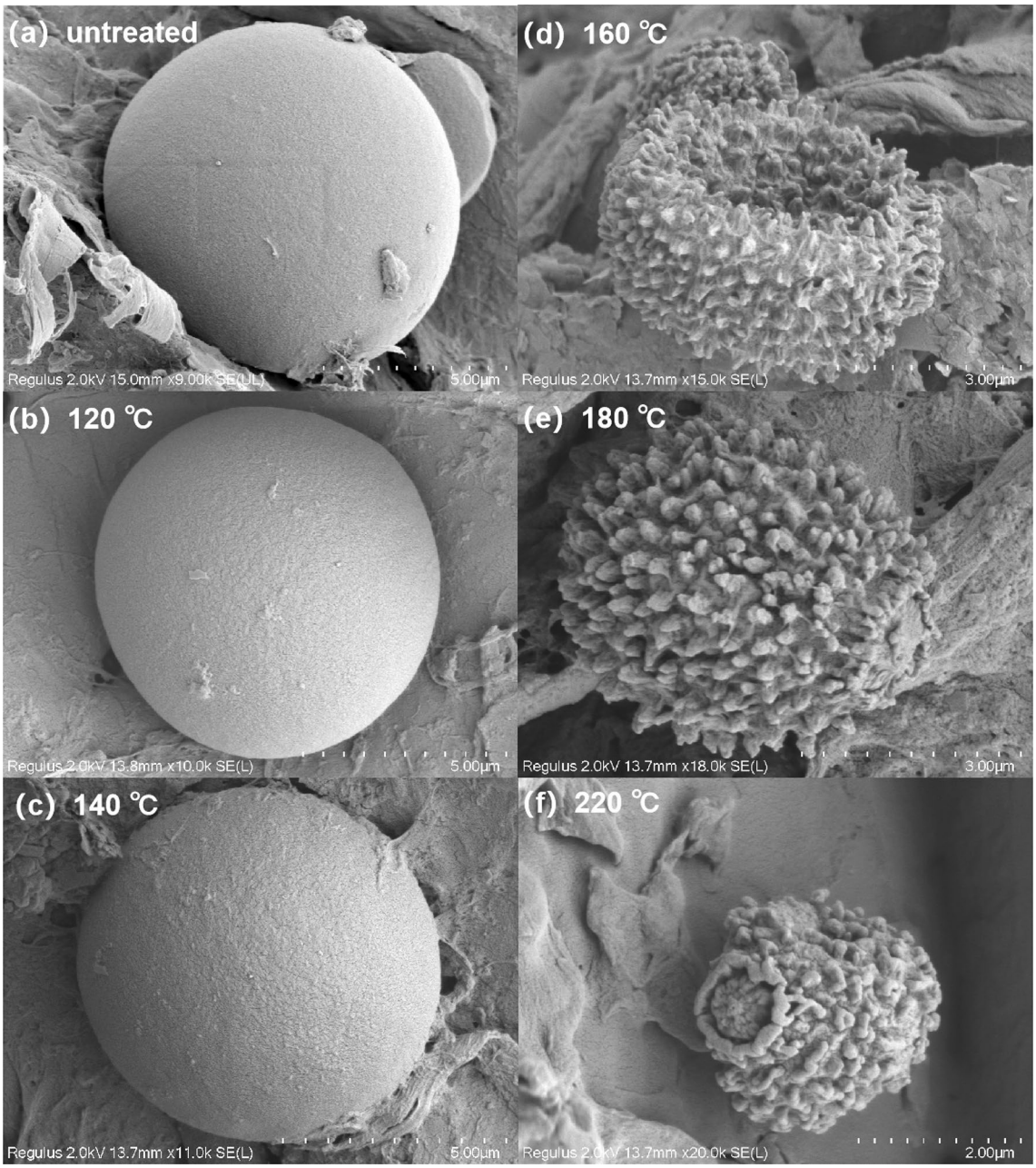

Fig. 5 SEM images of starch granules in the untreated- and treated parenchyma cells

high-pressure treatment. The varieties in the morphology and shape might be due to the differences in chemical composition and structure between starch in parenchyma cells and the starch granules in glutinous rice and corn, which need to be further investigated in the future. Moreover, the changes in starch granules may partly account for the improvement in the mold and decay resistance of bamboo treated by heat [26, 27].

Chemical composition

FTIR spectra of fibers and parenchyma cells after heat treatments are displayed in Fig. 6. The band at around 1735 cm^{-1} was attributed to C=O stretching from hemicellulose [28, 29]. Moreover, the bands at about 1608 cm^{-1}, 1509 cm^{-1}, and 1462 cm^{-1} were due to the aromatic skeleton vibration in lignin [21, 30, 31]. The band around 1735 cm^{-1} in both untreated and treated fibers and parenchyma cells, but the intensity was

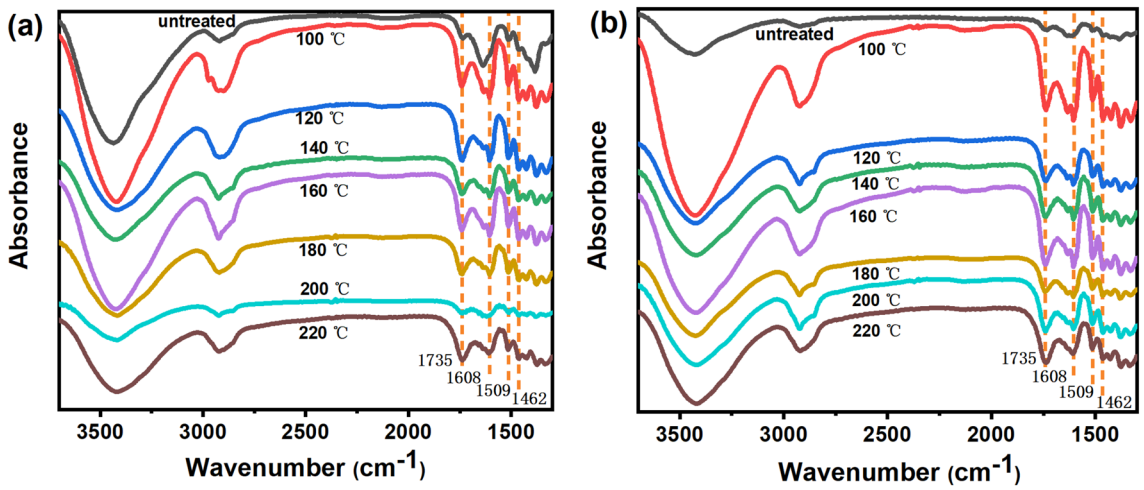

Fig. 6 FTIR spectra of **a** fibers and **b** parenchyma cells with heat treatments

different, suggesting the different content of hemicellulose. Besides, the intensity of the bands at 1608 cm^{-1} increased especially in the parenchyma cells after heat treatment suggesting that the content of lignin may increase. To get more insight into the change in chemical composition for heat-treated fibers and parenchyma cells, the contents of cellulose, hemicellulose, and lignin were quantitatively determined.

Figure 7 shows the chemical compositions of the untreated- and treated fibers and parenchyma cells. Bamboo fibers had higher cellulose content and lower hemicellulose content compared to parenchyma cells, which is in good agreement with previous research [15]. When treated by heat below 220 °C, the content of cellulose, hemicellulose, and lignin in both fibers and parenchyma cells almost did not change. However, when treated at 220 °C, the hemicellulose content decreased by 23% and 19% for fibers and parenchyma cells, respectively, while the content of lignin increased by 15% and 18%, respectively. The cellulose content of the 220 °C-treated fibers was similar to that of the untreated ones, but the cellulose content in the treated parenchyma cells increased by 15%. It indicated that 220 °C was a watershed of the change in chemical compositions of fibers and parenchyma cells, which was different from that in bamboo fibers treated with steam treatment. When bamboo fibers were treated with the 180 ℃ steam, the hemicellulose and cellulose content decreased substantially [32], indicating that water was another important factor affecting the chemical composition of bamboo when treated by the combination of heat and water.

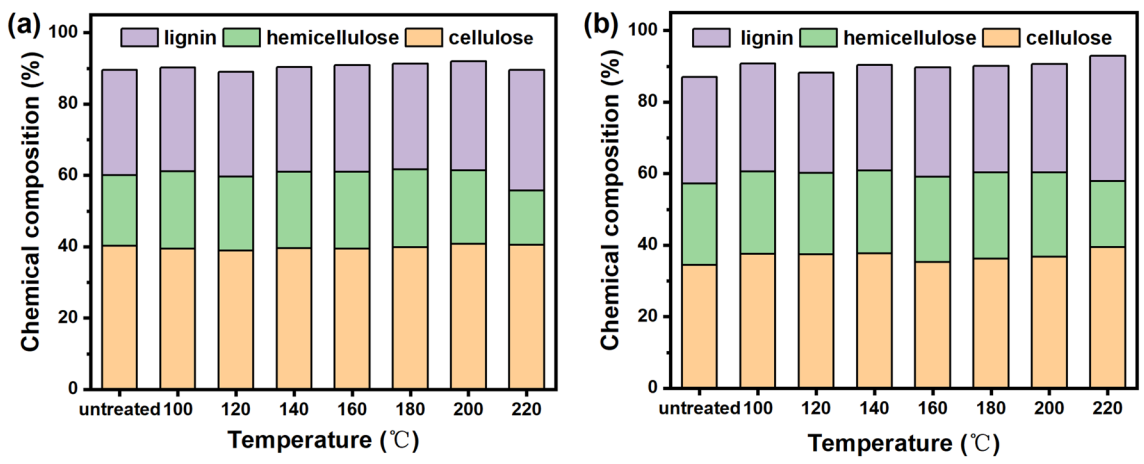

Fig. 7 Chemical compositions in **a** fibers and **b** parenchyma cells

The color changes of fibers and parenchyma cells are often associated with the content and chemical structure of lignin. The darkening color may be largely linked to the structural change of the lignin chromophore group as the temperature of heat treatment increased [33]. It was reported that the lignin structural monomer guaiac was demethylated to produce quinone compounds and the ether bond was broken, resulting in the darker color of fibers and parenchyma cells [18, 19, 34–36]. This was consistent with the color changes in fibers and parenchyma cells shown in Fig. 2 and Fig. 3.

X-ray diffraction

X-ray diffraction patterns of fibers and parenchyma cells treated at various heat temperatures are displayed in Fig. 8. The distinct peaks at 15.9°, 21.8°, and 34.7° corresponded to (1–10) and (110), (200), and (040) lattice planes, respectively [33], which is a characteristic for the typical cellulose I [37]. The patterns of the fibers and parenchyma cells treated by heat were the same as the cellulose I profile of the untreated one, suggesting that the heat treatment did not affect cellulose crystalline structure in both fibers and parenchyma cells.

Figure 9 shows the CrI values of fibers and parenchyma cells. The CrI of the untreated fibers was much higher than that of parenchyma cells, which was consistent with previous research [12, 15]. The CrI of fibers and parenchyma cells decreased when treated by heat regardless of the temperature used in this study. But among all the temperatures, the CrI of fibers and parenchyma cells treated at 100 °C decreased the most, and the fiber decreased more than parenchyma cell. It might be related to the water and the cellulose crystal form of bamboo fibers and parenchyma cell, which need be further studied in the future. It was reported that the crystallinity of Moso bamboo decreased after treated at 180 and 200 °C for 8 h [28], because of the partial degradation of the cellulose crystalline region. However, Yang et al. reported that the crystallinity of heat-treated Makino bamboo with 2 h remained unchanged at 180 °C but increased at 220 °C, which was in contrast with our results and it was probably due to the longer heat-treatment time used in our study [33]. A long time of heat treatment may have a negative influence on crystallinity [38].

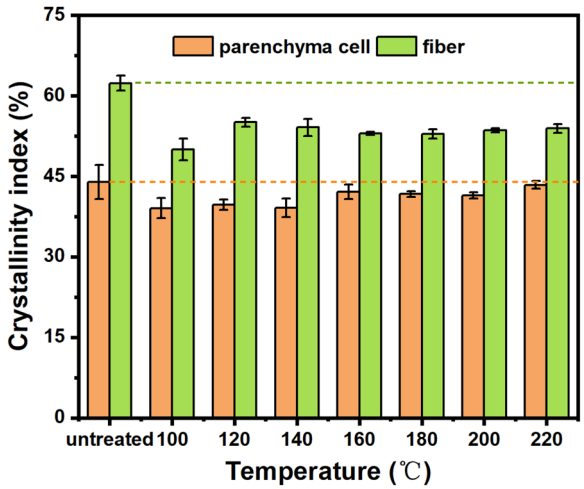

Fig. 9 The crystallinity index of cellulose in parenchyma cells and fibers

Thermal stability

Typical TGA and DTG curves of the untreated and treated fibers and parenchyma cells are displayed in Fig. 10. Three distinct weight-loss stages observed at 30–100 °C, 200–350 °C, 315–400 °C were mainly

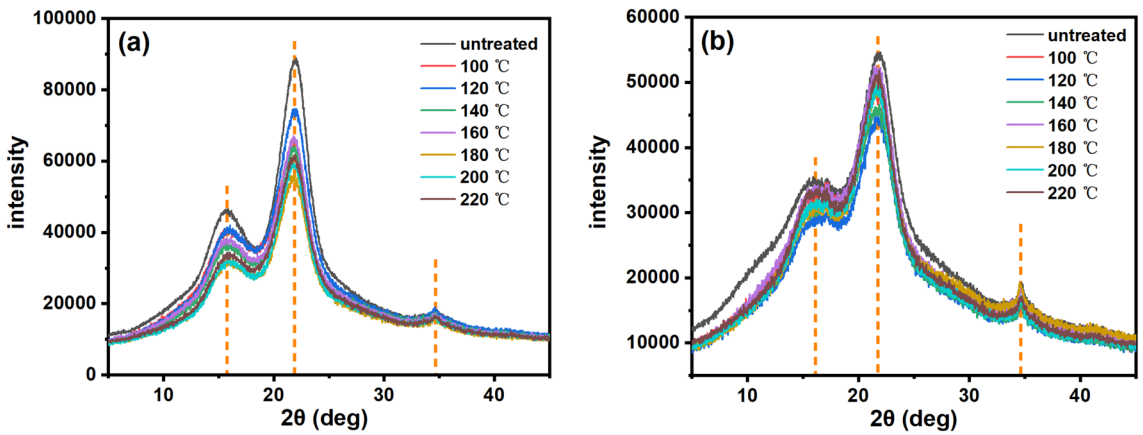

Fig. 8 XRD patterns of cellulose in **a** fibers and **b** parenchyma cells with heat treatments

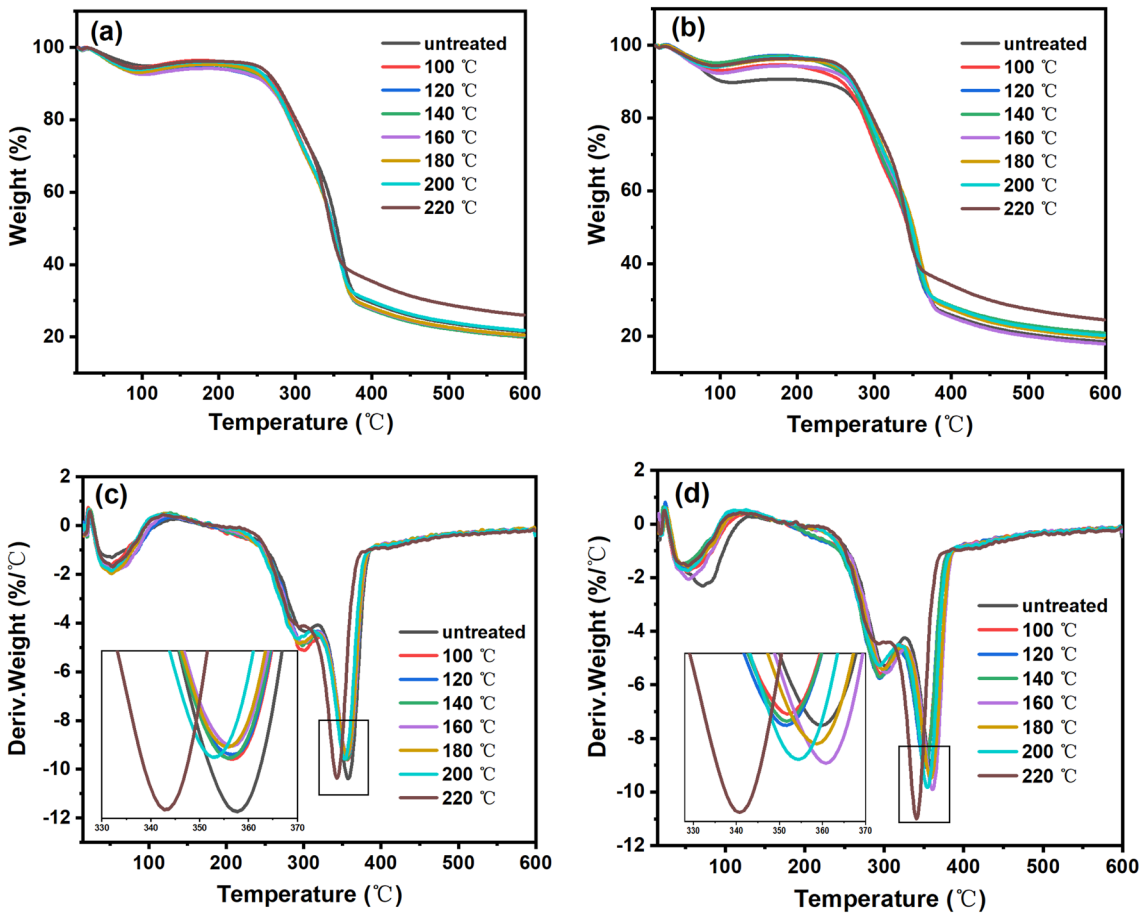

Fig. 10 Typical TGA curves of **a** fibers and **b** parenchyma cells, DTG curves of **c** fibers, and **d** parenchyma cells

attributed to the evaporation of water, the decomposition of hemicellulose, lignin, and cellulose, respectively. The shoulder peak observed at about 300 °C was caused by the thermal decomposition of hemicellulose. There was no significant change in the shoulder when the heat-treatment temperature was below 220 °C, but it was reduced obviously in fibers as well as parenchyma cells at 220 °C. It indicated that the content of hemicellulose decreased, which is consistent with the result of chemical composition analysis discussed previously.

The T_{max} value referred to the decomposition temperature corresponding to the maximum weight loss and related to maximum decomposition. The main peak at about 360 °C was caused by the thermal decomposition of cellulose in fibers and parenchyma cells (Fig. 10c, d). The cellulose chains in bamboo fibers were more closely packed and had smaller d-spacing than that of parenchyma cell cellulose [39]. It was the possible reason why the T_{max} of bamboo fibers was higher than that of parenchyma cells. The main peak of the fibers shifted to a lower temperature when treated at 200 and 220 °C, and the latter shifted more. The T_{max} of the heat-treated parenchyma cells decreased obviously except for the heat treatment at 160 °C. The T_{max} of parenchyma cells treated at 220 °C was the lowest. Lignin was more difficult to decompose than hemicellulose and cellulose [40, 41]. Lignin is a complex aromatic polymer composed of phenylpropane structural units connected by C–C bonds and C–O–C bonds. The bond energy was widely distributed, and the pyrolysis of lignin almost took place during the entire process [31], but the main degradation of lignin occurred at above 350 °C. The results revealed that the thermal stability of bamboo fibers remained almost unchanged at low treatment temperature but decreased at 200 or 220 °C, and the 220 °C-treatment resulted in the most pronounced decrease in thermal stability. For parenchyma cells, the decline of thermal stability was nearly the same when treated at 100–140 °C and it decreased with the increase of

temperature between 160 and 200 °C, but higher than that of 100–140 °C. The 220 °C-treatment decreased the most among all the temperatures.

Conclusions

In this study, the color, microstructure, chemical composition, and thermal stability of bamboo fibers and parenchyma cells with heat treatment were investigated. The results indicated that the heat-treatment temperature played a critical role in influencing fibers and parenchyma cells in terms of color, microstructure, chemical composition, and thermal stability. In addition, the difference in the change between the heat-treated parenchyma cells and the treated fibers was also compared:

(1) The colors of fibers and parenchyma cells were darkened after heat treatment, and the extent of the darkness between parenchyma cells and fibers treated with the heat at different temperatures was similar. In terms of microstructure, there was no insignificant change in fibers and parenchyma cells, but the starch granules surface was changed from smooth to spike-like shape when the temperature increased to 160 °C, and the number of starch granules with such shapes went up with increasing the heating temperature.

(2) Heat treatment affected the chemical composition of fibers and parenchyma cells depending on the temperature. The heat treatment below 220 °C almost did not change the chemical composition, but the chemical composition altered when treated at 220 °C. The cellulose content of the treated fibers was similar to that of the untreated one regardless of the temperature used, while the cellulose content for the 220 °C heat-treated parenchyma cells increased by 15%. The hemicellulose content of the treated fibers and parenchyma cells decreased while the lignin content increased when treated at 220 °C.

(3) The cellulose crystal structure in parenchyma cells and fibers after heat treatment still retained cellulose I form. The crystallinity index of the fiber was significantly reduced after heat treatment, while the CrI of the treated parenchyma cells decreased slightly.

(4) The effect of heat treatment on the thermal stability of parenchymal cells was more pronounced than that of fibers. The thermal stability of parenchyma cells was lower than that of fibers. The thermal stability of parenchyma cells decreased except for the treatment at 160 °C, and the highest treatment temperature led to the lowest thermal stability. The thermal stability for bamboo fibers decreased only when treated by heat at 200 and 220 °C.

Abbreviations

CrI: Crystalline Index; FT-IR: Fourier-transform infrared spectroscopy; SEM: Scanning electron microscopy; XRD: X-ray diffraction; TGA: Thermogravimetric analysis; DTG: Derivative thermogravimetry.

Supplementary Information

The online version contains supplementary material available at https://doi.org/10.1186/s10086-021-01988-2.

Additional file 1: Fig. S1. SEM images of starch granules in parenchyma cells treated at 160 ℃ and 180 ℃. **Fig. S2.** SEM images of starch granules in parenchyma cells treated at 200 ℃ and 220 ℃.

Acknowledgements

We thank Mr. Mingli Tao for helping prepare samples and doing some tests in this research.

Authors' contributions

WJY was the major contributor in data analysis and writing the manuscript. ZTH revised the manuscript. SJJ helped with the experiment and analyzed the data partly. FBH and ZWF financed the research. CH designed the experiment and participated in the writing. All authors read and approved the final manuscript.

Funding

This work was financed by the project funded by Zhejiang Province (2020SY09) and Key Laboratory of National Forestry and Grassland Administration/Beijing for Bamboo & Rattan Science and Technology in China (ICBR-2020-12) and China Postdoctoral Science Foundation (2020T130079).

Availability of data and materials

All data generated or analyzed during this study are included in this published article and its supplementary information files.

Declarations

Competing interests

The authors have declared no conflict of interests.

Author details

[1]College of Furnishings and Industrial Design, Nanjing Forestry University, Nanjing 210037, China. [2]Co-Innovation Center of Efficient Processing and Utilization of Forest Resources, Nanjing Forestry University, Nanjing 210037, China. [3]International Center for Bamboo and Rattan, Beijing 100102, China. [4]Zhejiang Academy of Forestry, Hangzhou 310023, China.

Received: 8 June 2021 Accepted: 27 September 2021
Published online: 12 October 2021

References

1. Yu T, Hu C, Chen X, Li Y (2015) Effect of diisocyanates as compatibilizer on the properties of ramie/poly(lactic acid) (PLA) composites. Compos A Appl Sci Manuf 76:20–27. https://doi.org/10.1016/j.compositesa.2015.05.010
2. Guo Y, Wang L, Wang H, Chen Y, Zhu S, Chen T, Luo P (2020) Properties of bamboo flour/high-density polyethylene composites reinforced with ultrahigh molecular weight polyethylene. J Appl Polym Sci 137:1–9. https://doi.org/10.1002/app.48971
3. Zhang J, Ning F, Kang M, Ma C, Qiu Z (2020) Effective removal of humic acid from aqueous solution using adsorbents prepared from the modified waste bamboo powder. Microchem J 153:104272. https://doi.org/10.1016/j.microc.2019.104272
4. Wang B, Lin F, hua, Zhao YY, Li XY, Liu YC, Li JB, Han XJ, Liu SX, Ji XR, Luo J, Wei YH, (2019) Isotactic polybutene-1/bamboo powder composites with excellent properties at initial stage of molding. Polymers 11:1–14. https://doi.org/10.3390/polym11121981
5. Lou CW, Lin CW, Lei CH, Su KH, Hsu CH, Liu ZH, Lin JH (2007) PET/PP blend with bamboo charcoal to produce functional composites. J Mater Process Technol 192–193:428–433. https://doi.org/10.1016/j.jmatprotec.2007.04.018

6. Ai T, Jiang X, Yu H, Xu H, Pan D, Liu Q, Chen D, Li J (2015) Equilibrium, kinetic and mechanism studies on the biosorption of Cu2+ and Ni2+ by sulfur-modified bamboo powder. Korean J Chem Eng 32:342–349. https://doi.org/10.1007/s11814-014-0227-8
7. Yu Y, Zhu R, Wu B, Hu Y, Yu W (2015) Fabrication, material properties, and application of bamboo scrimber. Wood Sci Technol 49:83–98. https://doi.org/10.1007/s00226-014-0683-7
8. Sharma B, Gatóo A, Ramage MH (2015) Effect of processing methods on the mechanical properties of engineered bamboo. Constr Build Mater 83:95–101. https://doi.org/10.1016/j.conbuildmat.2015.02.048
9. Chu J, Zhang J, Lu H (2016) Structural performance analysis of bamboo under different chemical and heat treatments. Trans Chin Soc Agric Eng 32:309–314. https://doi.org/10.11975/j.issn.1002-6819.2016.10.042
10. Meng FD, Yu YL, Zhang YM, Yu WJ, Gao JM (2016) Surface chemical composition analysis of heat-treated bamboo. Appl Surf Sci 371:383–390. https://doi.org/10.1016/j.apsusc.2016.03.015
11. Liese W, Köhl M (eds) (2015) Bamboo: the plant and its uses. Springer, Berlin
12. Jin K, Kong L, Liu X, Jiang Z, Tian G, Yang S, Feng L, Ma J (2019) Understanding the xylan content for enhanced enzymatic hydrolysis of individual bamboo fiber and parenchyma cells. ACS Sustain Chem Eng 7:18603–18611. https://doi.org/10.1021/acssuschemeng.9b04934
13. Lian C, Liu R, Zhang S, Yuan J, Luo J, Yang F, Fei B (2020) Ultrastructure of parenchyma cell wall in bamboo (*Phyllostachys edulis*) culms. Cellulose 27:7321–7329. https://doi.org/10.1007/s10570-020-03265-9
14. Zhang X, Huang H, Qing Y, Wang H, Li X (2020) A comparison study on the characteristics of nanofibrils isolated from fibers and parenchyma cells in bamboo. Materials 13:237. https://doi.org/10.3390/ma13010237
15. Chen H, Wu J, Shi J, Zhang W, Wang H (2021) Effect of alkali treatment on microstructure and thermal stability of parenchyma cell compared with bamboo fiber. Ind Crops Prod 164:113380. https://doi.org/10.1016/j.indcrop.2021.113380
16. Lian C, Zhang S, Liu X, Luo J, Yang F, Liu R, Fei B (2020) Uncovering the ultrastructure of ramiform pits in the parenchyma cells of bamboo [*Phyllostachys edulis* (Carr.) J. Houz.]. Holzforschung 74:321–331. https://doi.org/10.1515/hf-2019-0166
17. Wang X, Yuan Z, Zhan X, Li Y, Li M, Shen L, Cheng D, Li Y, Xu B (2020) Multi-scale characterization of the thermal–mechanically isolated bamboo fiber bundles and its potential application on engineered composites. Constr Build Mater 262:120866. https://doi.org/10.1016/j.conbuildmat.2020.120866
18. Chen Y, Tshabalala MA, Gao J, Stark NM, Fan Y (2014) Color and surface chemistry changes of extracted wood flour after heating at 120 ℃. Wood Sci Technol 48:137–150. https://doi.org/10.1007/s00226-013-0582-3
19. Ayadi N, Lejeune F, Charrier F, Charrier B, Merlin A (2003) Color stability of heat-treated wood during artificial weathering. Holz als Roh - und Werkstoff 61:221–226. https://doi.org/10.1007/s00107-003-0389-2
20. Sluiter A, Hames B, Ruiz R, Scarlata C, Sluiter J, Templeton D, Crocker LAPD (2008) Determination of structural carbohydrates and lignin in biomass. Lab Anal Proced 1617:1–16
21. Lee CH, Yang TH, Cheng YW, Lee CJ (2018) Effects of thermal modification on the surface and chemical properties of moso bamboo. Constr Build Mater 178:59–71. https://doi.org/10.1016/j.conbuildmat.2018.05.099
22. Shangguan W, Gong Y, Zhao R, Ren H (2016) Effects of heat treatment on the properties of bamboo scrimber. J Wood Sci 62:383–391. https://doi.org/10.1007/s10086-016-1574-3
23. Vallons KJR, Ryan LAM, Arendt EK (2014) Pressure-induced gelatinization of starch in excess water. Crit Rev Food Sci Nutr 54:399–409. https://doi.org/10.1080/10408398.2011.587037
24. Liu Z, Wang C, Liao X, Shen Q (2020) Measurement and comparison of multi-scale structure in heat and pressure treated corn starch granule under the same degree of gelatinization. Food Hydrocolloids 108:106081. https://doi.org/10.1016/j.foodhyd.2020.106081
25. Qiu C, Cao J, Xiong L, Sun Q (2015) Differences in physicochemical, morphological, and structural properties between rice starch and rice flour modified by dry heat treatment. Starch/Staerke 67:756–764. https://doi.org/10.1002/star.201500016
26. Cheng D, Jiang S, Zhang Q (2013) Mould resistance of Moso bamboo treated by two step heat treatment with different aqueous solutions. Eur J Wood Wood Prod 71:143–145. https://doi.org/10.1007/s00107-012-0654-3
27. Maria Silva Brito F, Benigno Paes J, da Silva T, Oliveira J, Donária Chaves Arantes M, Dudecki L (2020) Chemical characterization and biological resistance of thermally treated bamboo. Constr Build Mater 262:1–9. https://doi.org/10.1016/j.conbuildmat.2020.120033
28. Lin Q, Huang Y, Yu W (2020) An in-depth study of molecular and supramolecular structures of bamboo cellulose upon heat treatment. Carbohyd Polym 241:116412. https://doi.org/10.1016/j.carbpol.2020.116412
29. Li MF, Shen Y, Sun JK, Bian J, Chen CZ, Sun RC (2015) Wet Torrefaction of bamboo in hydrochloric acid solution by microwave heating. ACS Sustain Chem Eng 3:2022–2029. https://doi.org/10.1021/acssuschemeng.5b00296
30. Gao J, Qu L, Qian J, Wang Z, Li Y, Yi S, He Z (2020) Effects of combined acid-alkali and heat treatment on the physiochemical structure of Moso bamboo. Sci Rep 10:1–7. https://doi.org/10.1038/s41598-020-63907-7
31. Zhang Y, Yu Y, Lu Y, Yu W, Wang S (2021) Effects of heat treatment on surface physicochemical properties and sorption behavior of bamboo (*Phyllostachys edulis*). Constr Build Mater 282:122683. https://doi.org/10.1016/j.conbuildmat.2021.122683
32. Wang Q, Wu X, Yuan C, Lou Z, Li Y (2020) Effect of saturated steam heat treatment on physical and chemical properties of bamboo. Molecules. https://doi.org/10.3390/molecules25081999
33. Yang TC, Yang YH, Yeh CH (2021) Thermal decomposition behavior of thin Makino bamboo (*Phyllostachys makinoi*) slivers under nitrogen atmosphere. Mater Today Commun 26:102054. https://doi.org/10.1016/j.mtcomm.2021.102054
34. Englund F, Nussbaum RM (2000) Monoterpenes in Scots pine and Norway spruce and their emission during kiln drying. Holzforschung 54:449–456. https://doi.org/10.1515/HF.2000.075
35. Salim R, Wahab R, Ashaari Z (2009) Effect of oil heat treatment on chemical constituents of Semantan bamboo (*Gigantochloa scortechinii* Gamble). J Sustain Dev. https://doi.org/10.5539/jsd.v1n2p91
36. Huang X, Kocaefe D, Kocaefe Y, Boluk Y, Pichette A (2012) A spectrocolorimetric and chemical study on color modification of heat-treated wood during artificial weathering. Appl Surf Sci 258:5360–5369. https://doi.org/10.1016/j.apsusc.2012.02.005
37. French AD (2014) Idealized powder diffraction patterns for cellulose polymorphs. Cellulose 21:885–896. https://doi.org/10.1007/s10570-013-0030-4
38. Wang X, Cheng D, Huang X, Song L, Gu W, Liang X, Li Y, Xu B (2020) Effect of high-temperature saturated steam treatment on the physical, chemical, and mechanical properties of moso bamboo. J Wood Sci. https://doi.org/10.1186/s10086-020-01899-8
39. Ren W, Guo F, Zhu J, Cao M, Wang H, Yu Y (2021) A comparative study on the crystalline structure of cellulose isolated from bamboo fibers and parenchyma cells. Cellulose 28:5993–6005. https://doi.org/10.1007/s10570-021-03892-w
40. Yang H, Yan R, Chen H, Lee DH, Zheng C (2007) Characteristics of hemicellulose, cellulose and lignin pyrolysis. Fuel 86:1781–1788. https://doi.org/10.1016/j.fuel.2006.12.013
41. Li Y, Du L, Kai C, Huang R, Wu Q (2013) Bamboo and high density polyethylene composite with heat-treated bamboo fiber: thermal decomposition properties. BioResources 8:900–912. https://doi.org/10.15376/biores.8.1.900-912

Publisher's Note